

**Metamaterial particles for electromagnetic energy harvesting**

Omar M. Ramahi, Thamer S. Alnoneef, Mohammad Alshareef, and Muhammed S. Boybay

Citation: *Applied Physics Letters* **101**, 173903 (2012); doi: 10.1063/1.4764054

View online: <http://dx.doi.org/10.1063/1.4764054>

View Table of Contents: <http://scitation.aip.org/content/aip/journal/apl/101/17?ver=pdfcov>

Published by the [AIP Publishing](#)

---

**Advertisement:**



**Goodfellow**

metals • ceramics • polymers  
composites • compounds • glasses

**Save 5% • Buy online**  
70,000 products • Fast shipping

## Metamaterial particles for electromagnetic energy harvesting

Omar M. Ramahi,<sup>1,a)</sup> Thamer S. Almoneef,<sup>1,b)</sup> Mohammad Alshareef,<sup>1,c)</sup>  
and Muhammed S. Boybay<sup>2,d)</sup>

<sup>1</sup>*Department of Electrical and Computer Engineering, University of Waterloo, Waterloo, Ontario N2L 3G1, Canada*

<sup>2</sup>*Department of Computer Engineering, Antalya International University, Antalya, Turkey*

(Received 9 July 2012; accepted 11 October 2012; published online 22 October 2012)

Metamaterials are typically made of an ensemble of electrically small resonators such as metallic loops. The fact that such particles resonate individually to generate a bulk material behavior having enhanced constitutive parameters is essentially indicative of these particles' ability to collect energy. We show that such particles act as energy collectors when a resistive load is inserted within the particle's gap. A proof of concept is provided using a 5.8 GHz field and a split-ring resonator (SRR) as the electromagnetic energy collecting cell. Numerical simulation for a  $9 \times 9$  SRR array shows the effectiveness of an SRR array as an energy collector plate. © 2012 American Institute of Physics. [<http://dx.doi.org/10.1063/1.4764054>]

The advent of metamaterials brought unusual excitement into electromagnetic research. From the feasibility of cloaking in the microwave and visible frequency regimes to producing media with atypical permeability or permittivity profiles, metamaterials added new possibilities and exciting new engineering applications.<sup>1-3</sup> While the concept of a metamaterial is fundamentally based on assembling electrically small resonators to create a media with atypical electromagnetic properties, such resonators can vary in composition from dielectric spheres to simple wires constructed in different shapes and geometries. One such resonator that captured the interest of many researchers is the so-called split-ring resonator (SRR). The SRR is made of one or multiple broken loops where the loops are arranged concentrically. An example of a simple one-loop SRR is shown in Fig. 1.

If excited with an external field and specific frequency, the SRR resonates. The resonance of the SRR cell implies that at the exciting frequency, energy is stored within the resonator and oscillates between the electric and magnetic field in a manner highly similar to the resonance phenomenon in an RLC circuit operating at resonance. At the resonance frequency of the SRR, the electric or magnetic field (depending on the type of resonator) can lead to a build up of a relatively high field within the SRR region and especially a build up of the electric field within the gaps. The resonance frequency depends on the topology and dimensions of the SRR and on the substrate. Several analytic models were proposed to predict the resonance frequency with varying degrees of accuracy;<sup>4-7</sup> however, these models cannot be a substitute for full numerical modeling if highly accurate determination of the resonant frequency is desired. In earlier work,<sup>8</sup> the resonance strength, which is indicative of the intensity of the field build-up within the resonator, was shown to be dependent on the incident angle and polarization. This is indeed expected, as, for instance, in the case of an SRR (composed of either

single or multiple loops) the maximum magnetization takes place when the incident magnetic field is perpendicular to the SRR plane. However, what is not intuitive to these authors is that the intensity does not vary monotonically with the angle of the incident field.<sup>9</sup> Equally interesting is that the intensity of the resonance within an SRR cell present within an array structure is related to the polarization of the incident field in a complex fashion due to the interaction of the incident field with adjacent cells.

At resonance, the SRR exhibits a strong concentration of magnetic field within the SRR and a relatively high voltage across the gap. An SRR was designed using thin traces of microstrip lines to resonate at 5.8 GHz. Using an 0.79 mm thick Rogers Duroid RT5880 substrate, the dimensions of the SRR were optimized to achieve resonance at 5.8 GHz. The SRR resulting dimensions (see Fig. 1) were  $L = 5.9$  mm,  $w = 0.55$  mm, and  $g = 0.8$  mm. The SRR was designed using the full-wave three-dimensional electromagnetic fields simulator HFSS such that the scattering parameters indicate full reflection when a plane wave is incident normally on the SRR (the design procedure is omitted here for brevity but can be found in the literature such as Ref. 10). Fig. 2 shows the induced electric field distribution in the plane of the SRR when excited by a plane wave such that the magnetic incident field is normal to the plane of the SRR. Fig. 2 shows the electric field distribution at the resonant frequency of 5.8 GHz and at a slightly different frequency of 5.6 GHz. Notice how a slight shift in the resonant frequency leads to a dramatic drop in the gap voltage as exemplified by the intensity of the electric field at the gap. We need to emphasize, however, that the SRR in this numerical example is isolated. Had the SRR been part of an array structure, the field distribution on each SRR cell would be influenced by complex coupling from adjacent cells.

Since the gap is essentially an open circuit, the effective impedance seen by the current that is induced in the SRR loop is capacitive. In fact, at resonance, the SRR can be modeled as a voltage source in series with an RLC elements (see Ref. 11. Of course, the circuit model is valid outside the range of the SRR resonance, but the field build up is most

<sup>a)</sup>Electronic mail: oramahi@uwaterloo.ca.

<sup>b)</sup>Electronic mail: talmoneef@uwaterloo.ca.

<sup>c)</sup>Electronic mail: mohammed.alshareef@uwaterloo.ca.

<sup>d)</sup>Electronic mail: msboybay@uwaterloo.ca.

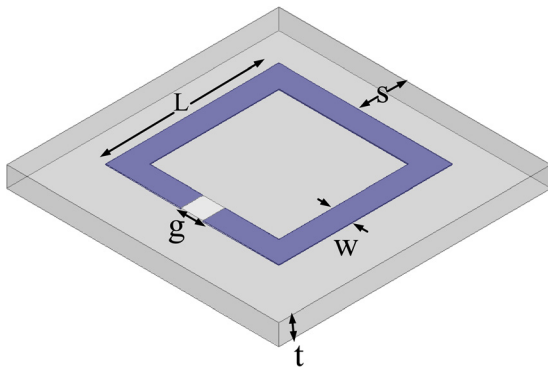


FIG. 1. Split ring resonator unit cell.

pronounced at resonance). Therefore, electromagnetic energy harvesting using the SRR cell can be possible by tapping on the field build up at the gap. This will be demonstrated here by placing a resistor within the gap of the SRR to mimic a power load. For the particular SRR used here, a resistance of  $2.3\text{ K}\Omega$  was found to yield maximum power absorption, implying highest power dissipation across the resistor when placed in the gap and when the field is incident such that the magnetic field is normal to the plane of the SRR. Of course, one would expect that the optimal load resistance would depend on the polarization of the incident field and the dimensions of the SRR. Such expectation is directly inferred from the work in Ref. 8. Additionally, the placement of a load resistor in the gap of the SRR created a slight shift in the resonant frequency which is of minor consequence since the SRR can always be redesigned to yield maximum load power absorption at the desired frequency.

We emphasize that the SRR is an electrically small resonator which makes it fundamentally different, as a receiver, from a classical antenna resonator. In the case of the antenna resonator operating as a receiver, the operation is effected very minimally by the load that is connected to the antenna terminals. In the case of electrically small resonators, such as an SRR, the mechanism is different as anything connected to the terminals of the resonator will affect the physical behavior of the resonator itself, especially in its ability to absorb

power from an incident electromagnetic field. Interestingly, traditional matching theories cannot be applied here in the classical sense since the maximum available power which develops within the SRR loop (according to Faradays law) is directly dependent on the gap and whatever is connected across it. Therefore, extracting the maximum power from the SRR without changing its topology or dimensions has to be done through optimization as we did in this work. However, in a future publication, we plan to explore the possibility of changing the topology of the SRR to maximize its power delivery.

Our objective here is purely to show the feasibility of the SRR to collect energy without being overly concerned with the polarization of the incident field. In fact, as we show below, when using an SRR array, energy can be effectively harvested when the polarization of the magnetic incident field is not necessarily normal to the plane of the SRR array. In a practical demonstration of the power harvesting capability of the SRR, which will be deferred to a later work, the gap resistor will be placed with a rectifying diode feeding a power grid.

An experiment was conducted to demonstrate the energy harvesting potential of a single SRR cell. An SRR was fabricated using identical material and dimensions to the one simulated above (aside from minor deviation typical of fabrication tolerances). The fabricated SRR was loaded with a  $2.7\text{ K}\Omega$  resistor, as shown in Fig. 3 since a single  $2.3\text{ K}\Omega$  resistor was not available at the time of the experiment.

The incident field was generated by a commercially available 19 dBi gain array antenna operating at the center frequency of 5.8 GHz with a matching bandwidth of 2.5 GHz. The transmitting antenna was positioned at a distance of 30 cm from the SRR such that the SRR was centered on a line normal to the plane of the transmitting antenna and emanating from its center. Fig. 4 illustrates the experiment setup. An Agilent Infiniium 91304ADSA 12 GHz oscilloscope equipped with a single-ended probe was used to record the voltage across the load resistor. As a result of the direct field excitation emanating from the high-gain antenna, a voltage of 611 mV was recorded across the gap resistor.

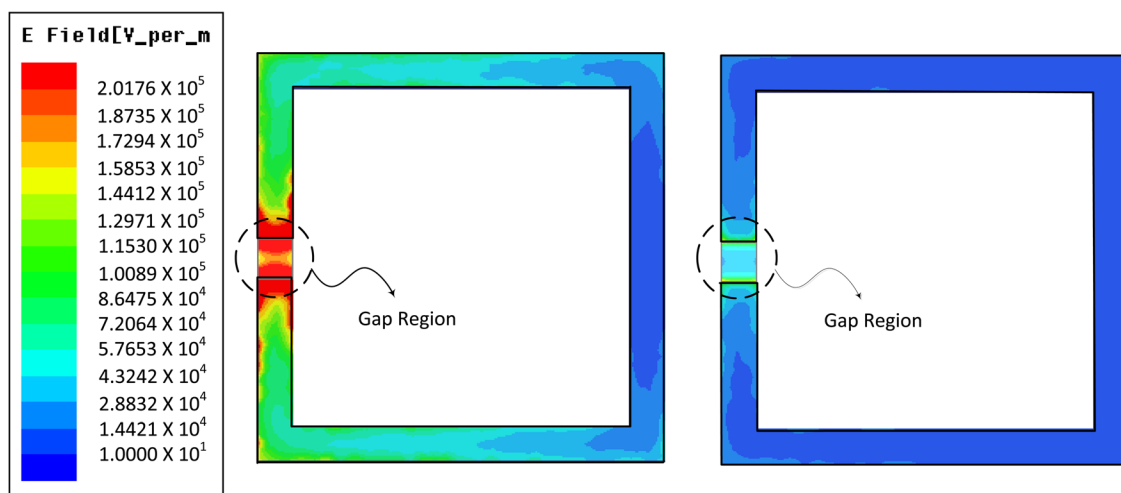


FIG. 2. Electric field distribution in the plane of the SRR. The SRR on the left is operating at the resonance frequency of 5.8 GHz, while the one on the right is at the frequency of 5.6 GHz. The scale ranges from 10 V/m (dark blue) to 201760 V/m (dark red).

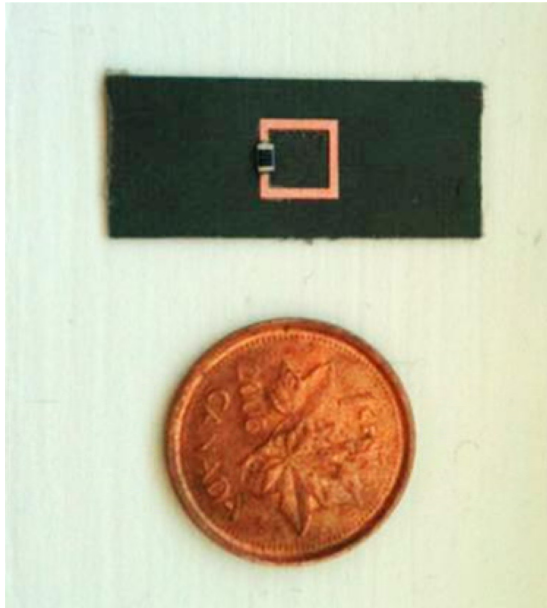


FIG. 3. Fabricated SRR with a 2.7 K $\Omega$  resistor placed in the gap.

In most previous works on the use of antennas for energy harvesting, which typically was referred to as rectenna research, a predominant goal was achieving high AC to DC conversion efficiency.<sup>12–14</sup> While the AC to DC conversion is important to the overall efficiency of the energy harvesting system, our immediate goal in this work is the microwave to AC conversion efficiency. In fact, an optimal AC to DC conversion link can be employed with any direct electromagnetic energy collector (i.e., antenna). What is missing from earlier work, however, is a relevant and meaningful definition of energy efficiency of the antenna or the energy collector, which we refer to in this work as *microwave to AC conversion efficiency*. By the microwave to AC conversion efficiency, we mean the efficiency of the

antenna to transfer the total power incident on a specific area to available power at the feed of the AC to DC link. This feed is shown as the a-b port in Fig. 5, which shows the schematic of a generic electromagnetic energy harvesting systems using an antenna and a rectifying diode. To calculate the microwave to AC conversion efficiency, we need to define a footprint, in square meters, occupied by the antenna system. Therefore, we introduce a definition for antenna system efficiency as  $\eta = P_{av}/P_{area}$ , where  $P_{av}$  is the maximum available time-average ac power received by the antenna or all antennas occupying the specific footprint under consideration and which is available at the feed terminal of the receiving antenna (terminal a-b in Fig. 5) and  $P_{area}$  is the total time-average power incident on the footprint. Notice that our definition here is not absolute in the sense that it is strongly dependent on the specific footprint (area) that is available for power harvesting. We stress here that the specific footprint of the antenna system considered here is not to be confused with the *effective area* of the antenna that is commonly used in antenna design as in Ref. 13.

In light of the power efficiency definition just established, we demonstrate the viability of the SRR array as an energy harvesting platform using full-wave numerical simulation. We consider an 85 mm  $\times$  85 mm footprint occupied by a 9  $\times$  9 SRR array (Fig. 6) resulting in a total of 81 SRR cells. Each SRR cell had a 2.3 K $\Omega$  placed in its gap, again, to mimic a power load. A horn antenna was used as the source of the incident field. Fig. 7 shows the positioning of the horn antenna with respect to the plane of the SRR array. While this numerical simulation is very costly in terms of simulation time and memory as the simulation domain is quite large, it avoids any potential contradiction arising from using a plane wave excitation (available in some commercial full-wave simulation tools) which mixes incident and total fields. The horn was positioned a distance of 120 cm from the center of the plate, as shown in Fig. 7, to insure that the incident

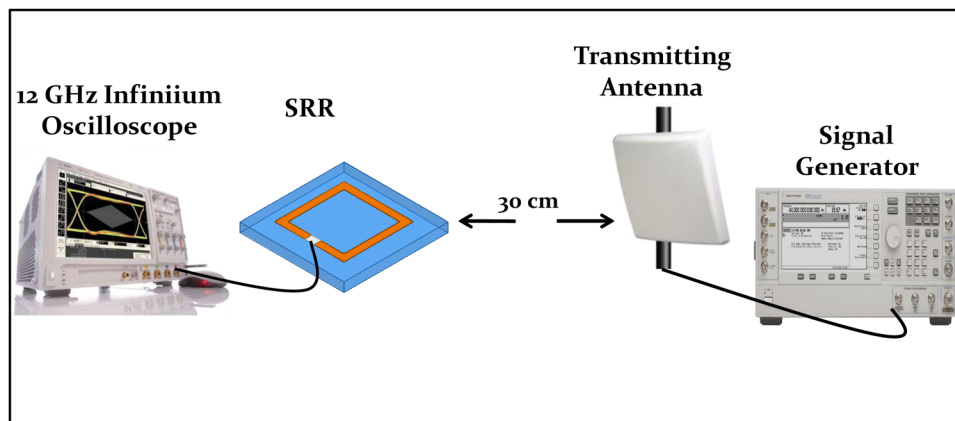


FIG. 4. Experimental setup used to measure the voltage induced across a resistor placed at the gap an SRR.

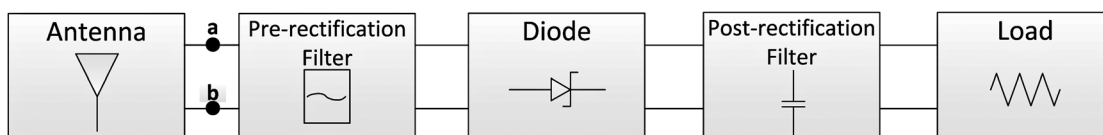
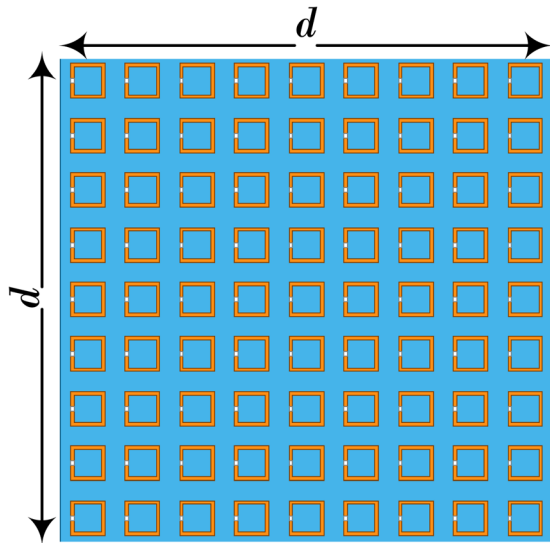


FIG. 5. A block diagram for a generic electromagnetic energy harvesting system employing an antenna as the primary collector.

FIG. 6. A  $9 \times 9$  SRR array plate.

field in close proximity of the SRR array plate is a traveling plane wave. Figure 8 shows the efficiency of the SRR array as a function of the frequency for different incident field angles  $\phi$ .  $P_{av}$  was calculated by summing the power dissipated in all 81 resistors.  $P_{area}$  was calculated by integrating the Poynting vector over the SRR array plate. We make several observations here. First, the smaller the angle  $\phi$ , the lower the efficiency. This is expected since the smaller the angle  $\phi$ , the smaller the incident magnetic field normal to the surface of the SRR. We also observe that the maximum efficiency varies with the frequency. In fact, we observed a sizeable bandwidth (exceeding 1.5 GHz) where the efficiency exceeds 40% for all three incident angles considered. This unexpectedly large bandwidth is most likely the result of the coupling between the SRR elements. We thus conclude that the SRR array can harvest energy over a relatively wide frequency band and over a wide range of incident field angles.

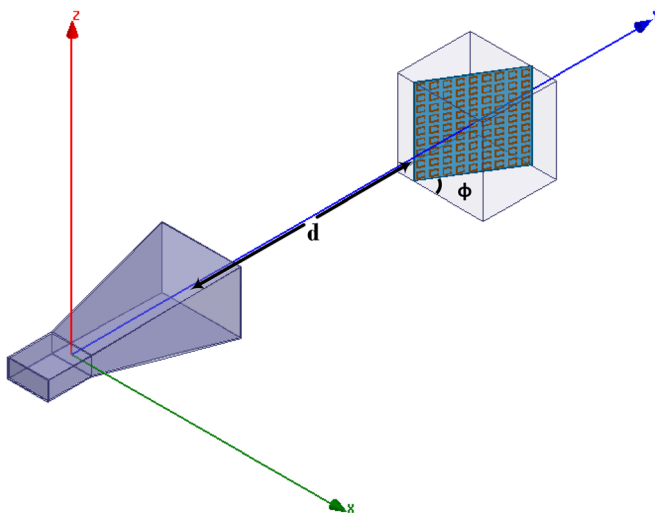
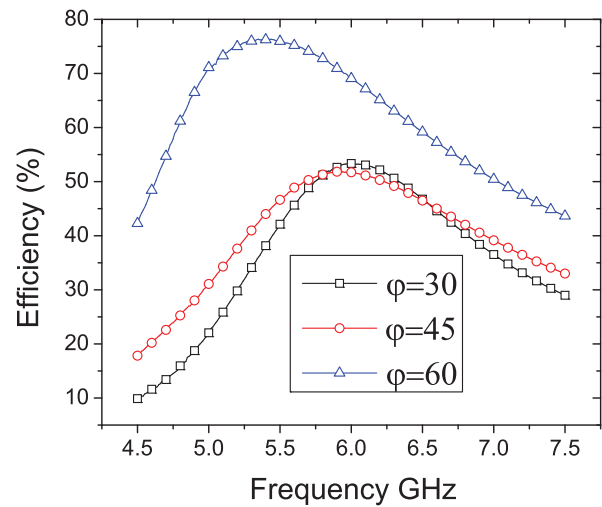


FIG. 7. Numerical simulation setup for electromagnetic energy collection using a horn antennas as the source of radiation and an SRR array as the collector.

FIG. 8. Energy harvesting efficiency of the  $9 \times 9$  SRR array for three different incident field angles  $\phi$  as described in Fig. 7.

We demonstrated the feasibility of using an SRR array to collect electromagnetic energy. We focused on a specific type of SRRs, but generalization can be made to other SRR structures. As a proof of concept, an optimal resistive load was placed in the gap of the SRR. The power dissipated in the resistor was indicative of the SRR potential to collect power. Preliminary simulations showed that the appropriately scaled SRRs can be used to harvest energy in sub-microwave or super-microwave frequency regimes. Future papers will report on these developments. Finally, we emphasize that the energy transfer mechanism presented here is based on far-field electromagnetic radiation which makes it fundamentally different from the mechanism of resonance inductive coupling reported in recent years.<sup>15</sup>

We like to acknowledge the support of the Natural Sciences and Engineering Research Council of Canada and the Saudi Arabian Ministry of Higher Education.

- <sup>1</sup>J. B. Pendry, "Negative refraction makes a perfect lens," *Phys. Rev. Lett.* **85**, 3966–3969 (2000).
- <sup>2</sup>J. B. Pendry, "Negative refraction," *Contemp. Phys.* **45**, 191–202 (2004).
- <sup>3</sup>N. I. Landy, S. Sajuyigbe, J. J. Mock, D. R. Smith, and W. J. Padilla, "Perfect metamaterial absorber," *Phys. Rev. Lett.* **100**, 207402 (2008).
- <sup>4</sup>R. Marqués, F. Mesa, J. Martel, and F. Medina, "Comparative analysis of edge- and broadside-coupled split ring resonators for metamaterial design: Theory and experiments," *IEEE Trans. Antennas Propag.* **51**, 2572–2581 (2003).
- <sup>5</sup>J. D. Baena, R. Marqués, F. Medina, and J. Martel, "Artificial magnetic metamaterial design by using spiral resonators," *Phys. Rev. B: Condens. Matter* **69**, 014402(1)–014402(5) (2004).
- <sup>6</sup>J. D. Baena, J. Bonache, F. Martn, R. M. Sillero, F. Falcone, T. Lopetegui, M. A. Laso, J. GarcaGarca, I. Gil, M. F. Portillo, and M. Sorolla, "Equivalent-circuit models for split-ring resonators and complementary split-ring resonators coupled to planar transmission lines," *IEEE Trans. Microwave Theory Tech.* **53**, 1451–1460 (2005).
- <sup>7</sup>V. Zhurbenko, T. Jensen, V. Krozer, and P. Meincke, "Analytical model for double split ring resonators with arbitrary ring width," *Microwave Opt. Tech. Lett.* **50**, 511–515 (2008).
- <sup>8</sup>P. Gay-Balmaz and O. J. F. Martin, "Electromagnetic resonances in individual and coupled split-ring resonators," *J. Appl. Phys.* **92**, 2929 (2002).
- <sup>9</sup>M. Quinten, *Optical Properties of Nanoparticle Systems: Mie and Beyond* (Wiley-VCH, 2011).
- <sup>10</sup>K. Aydin, I. Bulu, K. Guven, M. Kafesaki, C. M. Soukoulis, and E. Ozbay, "Investigation of magnetic resonances for different split-ring resonator parameters and designs," *New J. Phys.* **7**, 168 (2005).

- <sup>11</sup>L. Yousefi and O. M. Ramahi, "Artificial magnetic materials using fractal Hilbert curves," *IEEE Trans. Antennas Propag.* **58**, 2614–2622 (2010).
- <sup>12</sup>Y. J. Ren, M. F. Farooqui, and K. Chang, "A compact dual-frequency rectifying antenna with high-orders harmonic-rejection," *IEEE Trans. Antennas Propag.* **55**, 2110–2113 (2007).
- <sup>13</sup>N. Zhu, R. W. Ziolkowski, and H. Xin, "A metamaterial-inspired, electrically small rectenna for high-efficiency, low power harvesting and scavenging at the global positioning system L1 frequency," *Appl. Phys. Lett.* **99**, 114101 (2011).
- <sup>14</sup>B. Strassner and K. Chang, "5.8-GHz circularly polarized rectifying antenna for wireless microwave power transmission," *IEEE Trans. Microwave Theory Tech.* **50**, 1870–1876 (2002).
- <sup>15</sup>A. Kurs, A. Karalis, R. Moffatt, J. J. Dionopoulos, P. Fisher, and M. Soljacic, "Wireless power transfer via strongly coupled magnetic resonances," *Science* **317**, 83–86 (2007).